Journal of Alloys and Compounds, 197 (1993) 1–5
JALCOM 627

Synthesis and structure of two phases with both extended and point defects: $Mn_{1-x}Bi_{2+y}S_4$ and $Mn_{1-x}Bi_{2+y}Se_4$

Stephen Lee, Ernest Fischer, Jeff Czerniak and N. Nagasundaram
Department of Chemistry, University of Michigan, Ann Arbor, MI 48109-1055 (USA)

(Received June 17, 1992)

Abstract

We report the structures of $Mn_{1-x}Bi_{2+y}S_4$ ($0 \leqslant x \leqslant 0.3$; $y = 0.667x$) and $Mn_{1-x}Bi_{2+y}Se_4$ ($0.1 \leqslant x \leqslant 0.14$; $y = 0.667x$). Both compounds are defect structures of the $HgBi_2S_4$ structure type. In the case of $Mn_{0.7}Bi_{2.2}S_4$ we report a single crystal structure. The cell parameters are $a = 12.869(2)$ Å, $b = 3.9546(6)$ Å, $c = 14.771(2)$ Å, $\beta = 116.690(9)°$ and the space group is $C2/m$. Final refinement gave the values $R/R_w = 3.3/3.7\%$. This crystal was grown in an alkali halide flux. The reported compounds belongs to the family of chemically twinned face-centered cubic (f.c.c.) structures. Unlike most members of this family, they exhibit both extended defects and point defects.

1. Introduction

One recent theme in crystal chemistry is the interplay between crystalline defects and extended superstructures [1]. A family in which this interplay takes on striking form is the lead and bismuth sulfides or sulfosalts [2]. In these compounds, defects appear as glide reflection twinning planes. The $Mn_{1-x}Bi_{2+y}S_4$ and $Mn_{1-x}Bi_{2+y}Se_4$ ($y = 0.667x$) compounds reported in this paper have structures which belong to this family. These compounds have particular interest in that, unlike other members of this family, they contain both extended defects which change the overall space group symmetry and point defects which cause no change in the long-range order of the materials. Indeed, these compounds test our understanding that it is the exact stoichiometry which solely controls the type of glide twinning superstructure present in crystalline solids.

2. Experimental details

Both the $Mn_{1-x}Bi_{2+y}S_4$ and $Mn_{1-x}Bi_{2+y}Se_4$ compounds were prepared from mixtures of the elements. In general, all mixtures were prepared such that the overall stoichiometry of the reaction was $Mn_aBi_bQ_{a+1.5b}$ (Q ≡ S, Se). This initial composition corresponds to having respective oxidation states for the Mn, Bi and Q atoms of +2, +3 and −2. Reactions were carried out in sealed evacuated quartz tubes with 1–2 g samples. We heated the tubes slowly to final temperatures which ranged from 600–1000 °C (100–200 °C/day) and then annealed the sample at that temperature for several days. Room temperature powder X-ray investigations showed the appearance of new ternary phases. (A previous study [3] reported the existence of a tetragonal $MnBi_2Se_4$ phase (cell volume, 319 Å^3) but we were unable to find this in the current work.) However, repeated attempts to produce single crystals of these ternary phases by vapor transport techniques (using I_2 or Br_2 as transport agent) failed to produce suitable crystals for X-ray study. Indeed, all crystals isolated by vapor transport methods proved to be of the Bi_2Q_3 type. The implication is that, at the temperatures required for crystal growth by vapor transport, these ternary phases decompose. Finally, we were able to isolate single crystals of the ternary compounds using a lower temperature flux for crystal growth. The flux we used was an LiCl–RbCl (45% LiCl, 55% RbCl) eutectic mixture (which melts at 312 °C) [4]. Good crystals were obtained when the reaction mixture was cooled over a 1–2 week period from 800 to 400 °C. Generally 2–3 g of flux were included in these flux syntheses.

The final product was washed with water to remove all salt. It should be noted that the use of alkali metal halide fluxes to grow chalcogenides is somewhat unusual. Such solvents are generally used in oxide crystal growth [5a] and for hard cation sulfide phases, *e.g.* KI–KCl has been used to grow crystals of LaS_2 [5b]. However, it may well be that the use of hard cation–anion fluxes, such as alkali metal halides, may prove to be of general

0925-8388/93/$6.00

interest in soft cation–anion chalcogen crystal synthesis. This is so as only small levels of contamination of the relatively soft Mn–Bi chalcogenide by the hard LiCl and RbCl salts are found. A single crystal prepared by this flux method was first studied by Weissenberg techniques before being mounted on a four-circle diffractometer. Room temperature Guinier photographs (Enraf-Nonius camera) were taken using an Si standard. In the compounds reported in this paper the samples were further examined by electron microprobe to ensure the composition of the products (Cameca MBX automated electron microprobe with Kevex 8000 microanalyzer applied to single crystals). An independent chemical analysis was carried out for two samples (Galbraith Chemical). These latter analyses showed no trace of Li (less than 0.15%) in our final products.

3. Results

The compounds reported in this paper are all isostructural with $HgBi_2S_4$ [6]. In the case of manganese bismuth sulfides we were able to prepare this phase in or near the exact $MnBi_2S_4$ stoichiometry. It was also possible to prepare phases in which the metal content was defective with respect to this exact stoichiometry. In Table 1 we report the stoichiometry and cell constants for both the manganese bismuth sulfide and selenide phases. It should be noted that all attempts to prepare stoichiometric $MnBi_2Se_4$ failed. In this case we were only able to produce non-stoichiometric phases. Microprobe analyses on single crystals showed no trace of the elements of the flux medium (*i.e.* neither Rbn or Cl). Chemical analysis of the $Mn_{0.7}Bi_{2.2}S_4$ sample (from which the single crystal used in our X-ray structure determination was selected) showed 0.16% Rb, 0.69% Cl and no lithium (*i.e.* less than 0.15%). As the microprobe analysis shows no trace of Rb or Cl, the small quantities of these elements found in the chemical analyses could be due to the presence of a small amount of a second phase. The amount of such additional phases would perforce be quite small, as no extra products are observed in the X-ray powder analysis when the LiCl–RbCl flux is used. In this respect the salt flux reactions differ markedly from reactions without flux. In the non-flux reactions MnQ and Bi_2Q_3 are both observed, while in the flux reactions the ternary phases are produced quantitatively and without such impurities.

Analysis of the X-ray powder spectra is given in the supplementary material accompanying this paper (for data please write to authors). These X-ray analyses are complicated by the fact that the monoclinic cells are generally similar to the dimensions of a twofold larger end-centered orthorhombic cell. In the case of $Mn_{0.88}Bi_{2.08}S_4$ and $Mn_{0.90}Bi_{2.06}Se_4$ there is indeed a fusing of the monoclinic X-ray diffraction lines in a pseudo-orthorhombic pattern. Thus, for example the following pairs of reflections merge into each other in the aforementioned samples: (3,1,0)/(3,1,−3), (3,1,1)/(3,1,−4), (1,1,4)/(1,1,−5), (5,1,−5)/(5,1,0) and so forth. These four pairs of reflections are particularly important as their calculated intensities are very different from one another. For example the (3,1,1) reflection is six times stronger than the (3,1,−4) reflection in the case of $MnBi_2S_4$. We can therefore assign the correct unit cell (in samples in which the lines are distinct) due to our ability to associate the diffraction lines correctly within each of the above pairs.

It would appear that the pseudo-orthorhombic merging of the X-ray powder lines in the case of $Mn_{0.88}Bi_{2.08}S_4$ is not associated with the formation of a new structure type since no extra single crystal diffraction spots were observed at this stoichiometry. In addition, our solved structure is compatible only with a monoclinic cell. Finally, it may be seen that the evolution of the monoclinic β angle progresses in a steady fashion on going from $MnBi_2S_4$ (115.05°) to $Mn_{0.88}Bi_{2.08}S_4$ (115.69°) and $Mn_{0.70}Bi_{2.20}S_4$ (116.69°). Such a change in angle au-

TABLE 1. $Mn_{1-x}Bi_{2+y}Q_4$ (Q≡S, Se) phases and crystallographic cell constants

Compound	Microprobe analysis	Single crystal X-ray refinement	Starting composition	a (Å)	b (Å)	c (Å)	β (°)	Volume (Å^3)
$MnBi_2S_4$	$Mn_{0.139(3)}Bi_{0.287(10)}S_{0.574(10)}$	–	$Mn_{0.31}Bi_{0.15}S_{0.54}$	12.744(1)	3.9048(4)	14.735(1)	115.048(8)	664.27
$Mn_{0.88}Bi_{2.08}S_4$	$Mn_{0.125(4)}Bi_{0.294(1)}S_{0.581(4)}$	–	$Mn_{0.14}Bi_{0.26}S_{0.60}$ + LiCl–RbCl	12.799(2)	3.9268(5)	14.764(2)	115.69(1)	668.70
$Mn_{0.70}Bi_{2.20}S_4$	$Mn_{0.109(3)}Bi_{0.29(2)}S_{0.60(2)}$	$Mn_{0.102(1)}Bi_{0.320(2)}S_{0.58(1)}$	$Mn_{0.10}Bi_{0.31}S_{0.59}$ + LiCl–RbCl	12.869(2)	3.9546(6)	14.771(2)	116.690(9)	671.57
$Mn_{0.90}Bi_{2.06}Se_4$	$Mn_{0.119(4)}Bi_{0.29(1)}Se_{0.59(1)}$	–	$Mn_{0.14}Bi_{0.26}Se_{0.60}$ + LiCl–RbCl	13.357(1)	4.0730(3)	15.301(1)	115.887(8)	748.87
$Mn_{0.86}Bi_{2.09}Se_4$	$Mn_{0.114}Bi_{0.26}Se_{0.62}$	–	$Mn_{0.10}Bi_{0.31}Se_{0.59}$ + LiCl–RbCl	13.374(4)	4.081(1)	15.301(5)	116.26(2)	749.02

tomatically ensures the fusing of X-ray powder lines at some intermediate value and therefore there is no reason to believe that a true orthorhombic phase is formed.

In Table 2 the atomic positional parameters are listed for a single crystal of composition $Mn_{0.70}Bi_{2.20}S_4$. We refined this structure using, as an initial starting point, the atomic positions of the $HgBi_2S_4$ structure [6] for which Mn atoms were placed in the positions originally occupied by mercury atoms. The thermal parameters for one of the sites (site M in Table 2) were unusually small. We therefore allowed Bi atoms to also occupy the M site. We constrained the Bi and Mn occupations so that the M site was fully occupied. In the final stage of our refinement we allowed all other atomic occupation factors to refine. In the final refinement all thermal factors were found to be of near equal size (U_{eq} ranging from 0.014 to 0.022). The largest remaining peak in the Fourier difference map is a peak of 2.5 e $Å^{-3}$ which lies 0.90 Å away from a bismuth position. The final R/R_w value of the refinement is 3.3/3.7%. Bond distances are reasonable and are reported in Table 3. It can be seen in Table 3 and Fig. 3 (see below) that the metal atoms adopt either an octahedral environment (Bi1, M and Mn) or a distorted monocapped trigonal prism (Bi2). It is interesting that the Mn atom adopts a distorted octahedral environment with four coplanar short equatorial Mn–S bonds and two longer axial Mn–S bonds.*

The occupation factors of the various atomic positions lead to an overall stoichiometry of $Mn_{0.102(1)}Bi_{0.320(2)}S_{0.58(1)}$. This corresponds closely to the initial composition of the reaction mixture which was $Mn_{0.10}Bi_{0.31}S_{0.59}$. It can be seen that the charges of the cations and anions are balanced if we assign +2, +3 and −2 oxidation states to the Mn, Bi and S atoms respectively ($0.102\times2+0.320\times3=1.164\approx1.16=0.58\times2$). As it appears safe to assume that the oxidation states of the stoichiometric compound $MnBi_2S_4$ are also the same (as 1×2 (Mn)$+2\times3$ (Bi)$=8=4\times2$ (S)), we conclude that, over the entire range of stoichiometries found in $Mn_{1-x}Bi_{2+y}S_4$ ($0\leqslant x\leqslant0.3$), the oxidation states of the Mn, Bi and S atoms are constant. We therefore used the relative concentrations of the Mn and Bi atoms (as deduced from the microprobe analyses) to assign the nominal compositions of all the phases reported in Table 1.

TABLE 2. Parameters for $Mn_{0.7}Bi_{2.2}S_4$

Atom	x	y	z	Occupancy	U_{eq}
Bi1	0.21382(3)	0	0.36436(3)	0.990(4)	0.0191(2)
Bi2	0.35275(3)	0	0.13777(3)	1.004(4)	0.0190(2)
M[a]	0	0	0.5	1.00	0.0180(4)
Mn	0	0	0	0.79(1)	0.022(1)
S1	0.6602(2)	0	0.0418(2)	0.95(3)	0.0139(9)
S2	0.0112(2)	0	0.1724(2)	1.00(1)	0.0160(9)
S3	0.6020(2)	0	0.4422(2)	1.00(1)	0.0187(10)
S4	0.8204(3)	0	0.3136(2)	1.00(1)	0.022(1)

[a]M is 40.0(5)% Bi and 60.0(5)% Mn.

TABLE 3. Bond distances in $Mn_{0.7}Bi_{2.2}S_4$

Atom	Atom	Distance (Å)
Bi1	1S2	2.8363(2)
	1S3	2.774(2)
	2S3	2.965(3)
	2S4	2.698(3)
Bi2	1S1	2.582(3)
	2S1	2.984(2)
	2S2	2.719(2)
	2S4	3.431(2)
M (60% Mn/40% Bi)	4S3	2.714(2)
	2S4	2.684(2)
Mn	4S1	2.720(2)
	2S2	2.480(3)

4. Discussion

The $MnBi_2S_4$ structure is a member of the family of structures which have glide plane twinned cubic closest packed arrangements. These structures have been extensively reviewed [1, 2]. It is useful to summarize briefly the overall findings.

The parent structure for the entire family is the NaCl structure. This structure has a cubic closest packed array of Cl atoms in which all the octahedral holes are filled. It is important to note that MnS adopts the NaCl structure. The glide plane twinning is best understood when the MnS structure is viewed down the [110] crystallographic axis. This is shown in Fig. 1. It can be seen that the sulfur atoms lie at either height 0 or height ½. Sulfur atoms at any given height form infinite linear chains. These chains are shown at the top of Fig. 1. At the bottom of Fig. 1 we show that these chains together form sulfur octahedra which are filled with Mn atoms.

*It should be noted that a D_{4h} distortion close to that observed here is well known for Mn(III). However, this oxidation state is not compatible with the stoichiometry derived from either our single crystal X-ray work or the microprobe analysis. It should also be noted that the Mn(III) D_{4h} distortion generally has four short and two long bonds [7]. We therefore do not believe that the distortion in the Mn environment in $Mn_{0.7}Bi_{2.2}S_4$ is due to an Mn(III) Jahn–Teller effect. Furthermore, it has been noted (by the referee of this paper) that the short Mn–S bond is to the four coordinate S2 atom while the longer Mn–S bond is to the five coordinate S1 atom. This increase in coordination number should induce a change in bond length of the type observed here.

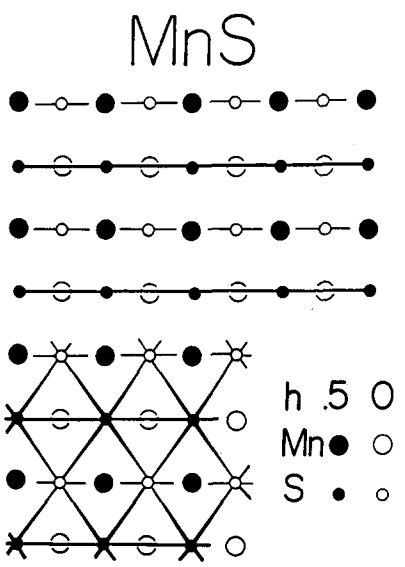

Fig. 1. The MnS structure (NaCl structure type) viewed down the [110] crystallographic axis. At the top of this figure we emphasize the infinite linear chains of atoms running in the horizontal direction. Underneath we show the sulfur octahedra present in the crystal.

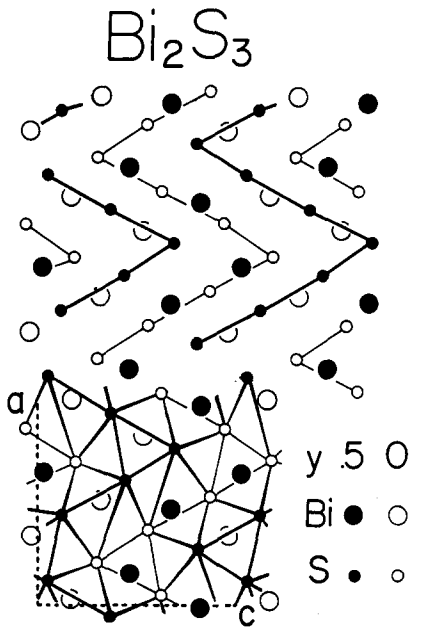

Fig. 2. The Bi_2S_3 structure (Sb_2Se_3 structure type) viewed down the [010] crystallographic axis. At the top of this figure we emphasize the infinite zigzag chains of atoms. At the bottom we emphasize the distorted octahedral and monocapped trigonal prismatic environments of the Bi atoms. The octahedra are highly distorted in this picture. In the case of the monocapped trigonal prisms the Bi atom has shifted away from the center of the trigonal prism to allow closer approach to the capping S atom.

In Fig. 2 we show the structure of Bi_2S_3, the other binary sulfide which is relevant to this study. It can be seen that the infinite linear chains present in the MnS structure have now taken on a zig-zag form (see the top portion of Fig. 2). As the number of sulfur atoms that remain in a single line segment is three, this zigzag pattern is generally called (3,3). It has been discussed [2] that this (3,3) zigzag pattern can be related to the change in stoichiometry on going from MnS to Bi_2S_3. To understand this it should be noted that each zig or zag converts two octahedra into three tetrahedral and a trigonal prism. The tetrahedral sites are small and remain unoccupied. Thus the overall number of available cation sites is reduced by the zigzag pattern. If the average length of the zigzag line segments is n then the ratio of cation sites to anion sites is $(n-1)$: n. For example, in the case of Bi_2S_3 the average zigzag line segment is $n=3$. This corresponds to the 2:3 stoichiometry found in these phases (as $n=3$ and hence $n-1=2$). Similarly, in the case of $MnBi_2S_4$ the average zigzag length should be $n=4$ as the ratio of cations to anions is 3:4. In Fig. 3 we show that this is indeed the case. The overall zigzag pattern for $MnBi_2S_4$ and $MnBi_2Se_4$ is in fact (5,3) (*i.e.* the (5,3) pattern has a value of $n=4$ as four is the average of five and three). It is of particular interest though, that this overall pattern is maintained even when the compound is quite defective in Mn. For example, in the case of the $Mn_{1-x}Bi_{2+y}S_4$ phases the overall ratio of cations to anions ranges from 0.75 to 0.725. By contrast, in the case of $Pb_{1-x}Bi_{2+y}S_4$ compounds there are three different compounds formed in this range. These are

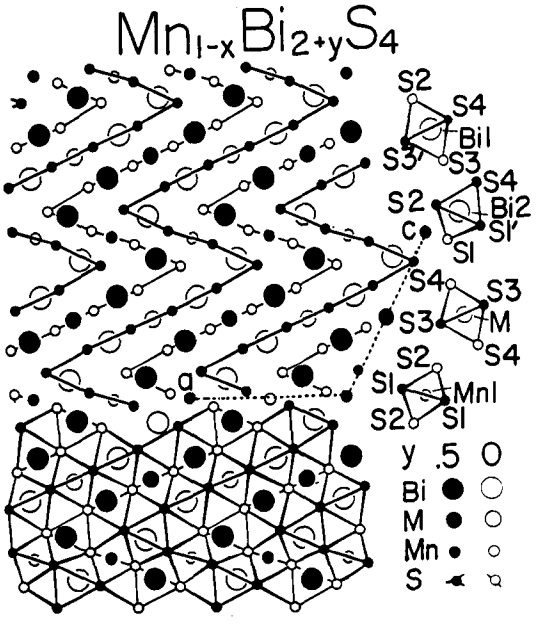

Fig. 3. The $Mn_{1-x}Bi_{2+y}S_4$ ($0 \leqslant x \leqslant 0.3$; $y=0.667x$) structure (defect $HgBi_2S_4$ structure type) viewed down the [010] crystallographic axis. At the top of this figure we emphasize the infinite zigzag chains of atoms and at the bottom we show the octahedral and monocapped trigonal prismatic arrangements of the sulfur atoms. Bond distances are given in Table 3. The similarity between the monocapped trigonal prismatic Bi atoms here and those of Bi_2S_3 shown in Fig. 2 should be noted.

$PbBi_2S_4$ (0.75 ratio), $Pb_2Bi_6S_{11}$ (0.727 ratio) and $Pb_3Bi_{10}S_{18}$ (0.722 ratio) [8]. In the lead bismuth sulfides there are certain discrete line phases with fixed cation to anion ratios. Intermediate phases will then disproportionate into the neighboring line phases in the PbS–Bi_2S_3 phase diagram. By contrast the MnS–Bi_2S_3 phase diagram is (at least at the temperature of crystal formation) not composed of compounds with a precise stoichiometry. Instead there is an interplay of extended defects, which lead to specific zigzag line segments, and point defects which allow play within a given structure type.

Acknowledgments

We wish to thank Dr. Jeff Kampf for recording the single crystal X-ray data set and the Petroleum Research Fund administered by the American Chemical Society for financial support of this research. We also wish to thank David Blake and Li Liang who prepared some of the reaction mixtures.

References

1 B. G. Hyde and S. Andersson, *Inorganic Crystal Structures*, Wiley, New York, 1989.
2 (a) B. G. Hyde, S. Andersson, M. Bakker, C. M. Plug and M. O'Keefe, *Prog. Solid State Chem., 12* (1980) 273. (b) H. H. Otto and H. Strunz, *N. Jb. Miner. Abh., 108* (1968) 1. (c) Y. Takéuchi and J. Takagi, *Proc. Jpn. Acad. Sci., 50* (1974) 843. (d) E. Makovicky, *N. Jb. Miner. Abh., 131* (1977) (e) E. Makovicky and S. Karup-Møller, *N. Jb. Miner. Abh., 130* (1977) 264; *131* (1977) 56.
3 P. G. Rustamov, S. A. Sadykhova and M. G. Safarov, *Russ. J. Inorg. Chem., 24* (1979) 787.
4 E. M. Levin, C. R. Robbins and H. F. McMurdie, *Phase Diagrams for Ceramists*, American Ceramic Society, Columbus, OH, 1964.
5 (a) D. Elwell and H. J. Scheel, *Crystal Growth from High Temperature Solutions*, Academic Press, London, 1975, Chapter 10. (b) J. Dugué, D. Carré and M. Guittard, *Acta Crystallogr. Sect. B, 34* (1978) 403.
6 W. G. Mumme and J. A. Watts, *Acta Crystallogr. Sect. B, 36* (1980) 1300.
7 F. A. Cotton and G. Wilkinson, *Advanced Inorganic Chemistry*, Wiley, New York, 4th edn., 1980, p. 743.
8 Y. Takéuchi, T. Ozawa and J. Takagi, *Kristallogr., 150* (1979) 75.